Influence of Reaction Conditions on the Synthesis of Self-Cross-Linked *N*-Isopropylacrylamide Microgels

Jun Gao and Barbara J. Frisken*

Department of Physics, Simon Fraser University, Burnaby, British Columbia V5A 1S6, Canada

Received February 6, 2003. In Final Form: April 3, 2003

We report systematic investigations of the reaction conditions necessary for the production of self-cross-linked poly(*N*-isopropylacrylamide) (PNIPAM) microgel particles. Reaction temperatures (T_{syn}) ranging from 40 to 90 °C and various monomer (C_{NIPAM}) and initiator (C_{KPS}) concentrations were investigated. Laser light scattering was used to characterize the resultant gel particles at 25 and 40 °C, below and above the phase transition temperature of PNIPAM. By comparing the molar masses measured at these two temperatures, well-defined ranges of T_{syn}, C_{NIPAM}, and C_{KPS} were found in which the polymer chains were well self-cross-linked and formed gel networks. Variations in the size and solid density as a function of these parameters are also discussed.

Introduction

Since the first synthesis of poly(*N*-isopropylacrylamide) (PNIPAM) microgels in 1986,[1] these particles have become by far the most widely investigated water-based, temperature-sensitive microgels.[2,3] PNIPAM-based microgels are temperature-sensitive because PNIPAM undergoes a volume phase transition at a lower critical solution temperature (LCST) of around 33 °C.[4] There is a growing interest in these materials because of potential applications as building blocks for more complicated structures,[5−7] as temperature-sensitive vessels,[8] and in permeable membranes[9] for controlled drug release.

The standard technique used to form PNIPAM microgels[1,10] is precipitation polymerization. A solution consisting of the *N*-isopropylacrylamide (NIPAM) monomer and cross-linker is heated to temperatures well above the LCST of PNIPAM, and an initiator is introduced. Because the growing PNIPAM chains are very hydrophobic at these temperatures, they collapse into nano-aggregates mainly stabilized by charged groups originating from an ionic initiator or added ionic surfactant. In most cases of PNIPAM microgel synthesis, a monomer containing two vinyl groups, *N*,*N*′-methylenebisacrylamide (BIS), is used to cross-link the polymer chains into polymer networks. However, the use of a chemical cross-linker can lead to structural inhomogeneities[11−13] if the reaction rate of the cross-linker is different from that of the monomer, as is known for BIS.[14]

We recently observed the formation of PNIPAM microgel particles during synthesis under reaction conditions that were normal except for the absence of an added cross-linker. We showed that NIPAM can self-cross-link into microgel particles through tert carbon atoms both during and after the polymerization of the NIPAM monomers.[15] These stable microgels, with radii of several hundred nanometers, molar masses as high as 10^9 g/mol, and solid densities as low as 0.013 g/cm^3 at 25 °C in water, resemble normal BIS-cross-linked PNIPAM microgels in every aspect, including the formation of a colloidal crystalline structure at suitable volume fractions. The kinetics of self-cross-linking and exclusion of pure hyperbranching as a source of formation of PNIPAM particles were also presented in our previous paper.[15]

In this work, we describe the systematic synthesis of PNIPAM microgels without the use of an added cross-linker carried out under different reaction conditions. By using laser light scattering to characterize the sizes and molar masses of the resultant gel nanoparticles, suitable conditions were found for effective self-cross-linking. In general, the aggregates have to reach a sufficiently high solid density to ensure that interchain cross-linking can occur. The extent of intrinsic self-cross-linking was also estimated by comparing the density of these particles with that of particles made with an added cross-linker. These studies of the influence of the reaction temperature and initial monomer and initiator concentrations on the resultant particle sizes, molar masses, and densities also provide insight into BIS-cross-linked NIPAM microgel synthesis.

Materials and Method

Synthesis of Gel Nanospheres. NIPAM from Acros Organics (Geel, Belgium) was recrystallized from hexane/acetone solutions. BIS and potassium persulfate (KPS) from Aldrich were used as

* Corresponding author. E-mail: frisken@sfu.ca.

(1) Pelton, R. H.; Chibante, P. *Colloids Surf.* **1986**, *20*, 247.
(2) Saunders, B. R.; Vincent, B. *Adv. Colloid Interface Sci.* **1999**, *80*, 1.
(3) Pelton, R. H. *Adv. Colloid Interface Sci.* **2000**, *85*, 1.
(4) Hirokawa, Y.; Tanaka, T. *J. Chem. Phys.* **1984**, *81*, 6379.
(5) Hu, Z.; Lu, X.; Gao, J.; Wang, C. *Adv. Mater.* **2000**, *12*, 1173. Hu, Z.; Lu, X.; Gao, J. *Adv. Mater.* **2001**, *13*, 1708.
(6) Jones, C. D.; Lyon, L. A. *Macromolecules* **2000**, *33*, 8301.
(7) Zha, L.; Zhang, Y.; Yang, W.; Fu, S. *Adv. Mater.* **2002**, *14*, 1090.
(8) Leobandung, W.; Ichikawa, H.; Fukumori, Y.; Peppas, N. A. *J. Controlled Release* **2002**, *80*, 357.
(9) Zhang, K.; Wu, X. Y. *J. Controlled Release* **2002**, *80*, 169.
(10) McPhee, W.; Tam, K. C.; Pelton, R. H. *J. Colloid Interface Sci.* **1993**, *156*, 24.
(11) Norisuye, T.; Masui, N.; Kida, Y.; Ikuta, D.; Kokufuta, E.; Ito, S.; Panyukov, S.; Shibayama, M. *Polymer* **2002**, *43*, 5289.
(12) Guillermo, A.; Cohen Addad, J. P.; Bazile, J. P.; Duracher, D.; Elaissari, A.; Pichot, C. *J. Polym. Sci., Part B: Polym. Phys.* **2000**, *38*, 889.
(13) Fernandez-Barbero, A.; Fernandez-Nieves, A.; Grillo, I.; Lopez-Cabarcos, E. *Phys. Rev. E* **2002**, *66*, 051803.
(14) Wu, X.; Pelton, R. H.; Hamielec, A. E.; Woods, D. H.; McPhee, W. *Colloid Polym. Sci.* **1994**, *272*, 467.
(15) Gao, J.; Frisken, B. J. *Langmuir* **2003**, *19*, 5212.

10.1021/la034207s CCC: $25.00
Published on Web 05/23/2003

Table 1. Recipes for the Synthesis of Self-Cross-Linked NIPAM Gel Microspheres in Water

	synthesis		concentration (in 100 g of solution)		
batch no.	T (°C)	t (h)	$W_{NIPAM} + W_{BIS}$ (g)	KPS (mg)	n_{BIS}/n_{NIPAM} (%)
062	39 ± 0.5	15	1.00	40	0
055	42.5 ± 0.5	15	1.00	40	0
054	48.5 ± 0.5	15	1.00	40	0
053	53.5 ± 1.5	5.5	1.00	40	0
040	61.5 ± 1.5	6.0	1.00	40	0
009	70 ± 1	4.0	1.00	40	0
038	76.5 ± 1.5	2.5	1.00	40	0
045	80.5 ± 0.5	2.5	1.00	40	0
051	89 ± 1	2.5	1.00	40	0
034	70 ± 1	4.0	0.10	40	0
039	70 ± 1	4.0	0.50	40	0
009	70 ± 1	4.0	1.00	40	0
050	70 ± 1	4.0	1.50	40	0
058	70 ± 1	4.0	1.00	5	0
047	70 ± 1	4.0	1.00	10	0
046	70 ± 1	4.0	1.00	20	0
009	70 ± 1	4.0	1.00	40	0
048B	70 ± 1	4.0	1.00	77	0
035	70 ± 1	4.0	1.00	160	0
009	70 ± 1	4.0	1.00	40	0
063	70 ± 1	4.0	1.00	40	1.0
064	70 ± 1	4.0	1.00	40	2.0
049	70 ± 1	4.0	1.00	40	5.0

received. Fresh deionized water from a Milli-Q Plus water purification system (Millipore, Bedford; 0.2-μm filter) was used throughout this work. The NIPAM solution was stirred under a nitrogen atmosphere in a 150-mL reactor for ~30 min and heated to the required temperature using a digital heating plate and water bath covered with a thin layer of paraffin oil. A KPS/water solution was added to the reactor to initiate polymerization. The reaction system was stirred at the incubation temperature for a time sufficient to ensure that all of the monomer was exhausted. After being cooled to room temperature, the final reaction dispersion was ready for characterization. Table 1 contains the details of the reaction conditions used for the different samples prepared for this study.

Laser Light Scattering. The apparatus used for the light scattering measurements was an ALV-5000 spectrometer/goniometer equipped with a digital time correlator and a helium−neon laser.

We used static light scattering to measure the weight-average molar mass M_w and z-average root-mean-square radius of gyration R_g. For small particles, we used a standard Zimm plot analysis to find M_w and R_g from the Rayleigh ratio $R_{vv}(q)$, determined from the time-averaged scattered intensity[16]

$$\frac{KC}{R_{vv}(q)} \cong \frac{1}{M_w}\left(1 + \frac{1}{3}R_g^2 q^2\right) + 2A_2C \qquad (1)$$

where $K = 4\pi^2 n^2 (dn/dC)^2/(N_A \lambda_o^4)$, $q = (4\pi n/\lambda_o)\sin(\theta/2)$ is the scattering wave vector, and A_2 is the second virial coefficient, with N_A, n, C, λ_o, and θ being Avogadro's constant, the solvent refractive index, the concentration (g/mL), the light wavelength in a vacuum, and the scattering angle, respectively. The angular range at which these measurements were carried out was restricted to keep $qR \ll 1$. For PNIPAM, the values used for dn/dC were 0.167 and 0.174 mL/g at 25 and 40 °C, respectively.[17] It should be mentioned that, for most of the batches in Table 1, only one dilute sample from each batch at a concentration of ~10^{-5} g/mL was used in the static laser light scattering to obtain M_w and R_g. Because the samples are so dilute and A_2 in eq 1 is so small for PNIPAM in water,[18] the difference between M_w measured using only one dilute sample and that using a group of samples is negligible. For larger particles, we fit the data to the form

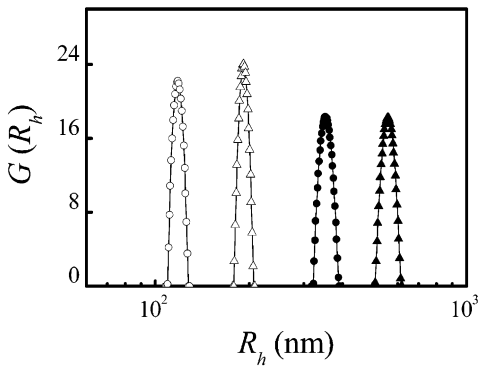

Figure 1. Normalized hydrodynamic radius distribution of self-cross-linked NIPAM microgels in water at 25 °C (solid symbols) and 40 °C (open symbols) for batch 053 (triangles, $C = 4.87 \times 10^{-5}$ g/mL) and batch 038 (circles, $C = 2.62 \times 10^{-5}$ g/mL), as was measured by DLS at scattering angles of 12 and 15° for batches 053 and 038 at 25 °C and at 30° for both batches at 40 °C.

$$\frac{KC}{R_{vv}(q, R)} = \frac{1}{M_w P(q, R)} \qquad (2)$$

where $P(q, R) = [3/(q^3R^3)(\sin(qR) - qR\cos(qR))]^2$ is the form factor for uniform spheres with radius R.

We used dynamic light scattering (DLS) to measure the time correlation function of the scattered intensity $g^2(\tau)$ as a function of the decay time τ. The DLS measurements were made at a scattering angle of $\theta = 30°$ unless otherwise noted. The samples were prepared by diluting the sphere dispersions to polymer concentrations of 10^{-5} g/mL. The hydrodynamic radius $\langle R_h \rangle$ and polydispersity of the samples were determined from analysis of $g^2(\tau)$ using either CONTIN[19] or cumulant analysis.[20] In general, the particle size distributions were very narrow with relative standard deviations of about 10%.

The solid density of the particles was calculated from the results of both static and DLS measurements. Previous studies have shown that PNIPAM microgel particles are spherical.[1,3] For spherical particles with a narrow particle size distribution, the solid density ρ can be calculated from the simple equation $M_w = {}^4/_3\pi\rho\langle R_h \rangle^3 N_A$.

Results and Discussion

Particle Characterization. Figure 1 shows the distribution of the hydrodynamic radii obtained by CONTIN analysis of the DLS data for samples from batches 053 (triangles) and 038 (circles) at 25 (solid symbols) and 40 (open symbols) °C, below and above the LCST of PNIPAM, which is typically around 33 °C. Below the LCST, the distributions are characterized by average hydrodynamic radii of 560 and 352 nm and small relative standard deviations of about 10%. The average radius decreases by a factor of 2.9, and the distributions become even narrower as the temperature is increased.

We also probed the particle structures by comparing the particle radii from the static measurements, which measure the particle size on the basis of the refractive index variations, and from the dynamic measurements, which measure the particle size on the basis of the hydrodynamic size. The ratios of $R_g/\langle R_h \rangle$ are between 0.8 and 1 at 25 °C and between 0.65 and 0.8 at 40 °C for all the particles measured, close to the theoretical value of 0.77 for uniform spheres.

(16) Zimm, B. H. *J. Chem. Phys.* **1948**, *16*, 1099.
(17) Gao, J.; Wu, C. *Macromolecules* **1997**, *30*, 6873.
(18) Gao, J.; Hu, Z. *Langmuir* **2002**, *18*, 1360.
(19) Provencher, S. W. *Makromol. Chem.* **1979**, *180*, 201; *Comput. Phys. Commun.* **1982**, *27*, 229.
(20) Chu, B. *Laser Light Scattering*; Academic Press: Boston, 1991.

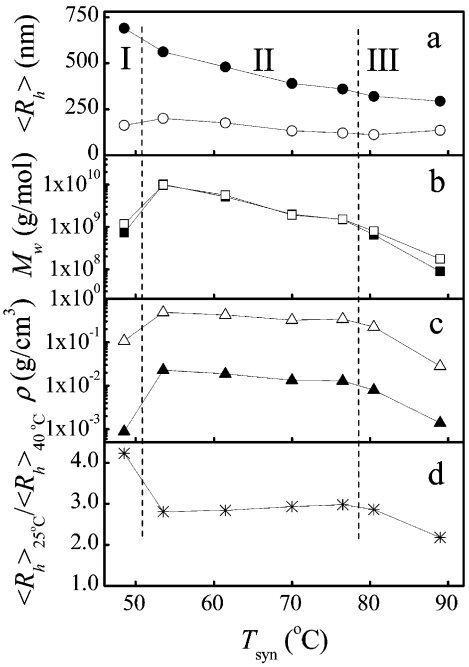

Figure 2. (a) *z*-average hydrodynamic radius $\langle R_h \rangle$, (b) weight-average molar mass M_w, (c) average solid density ρ, and (d) reduced size $\langle R_h \rangle_{25°C}/\langle R_h \rangle_{40°C}$ of particles produced as a function of the reaction temperature T_{syn} at a constant initial C_{NIPAM} of 10 g/L and an initial C_{KPS} of 400 mg/L. The solid and open symbols represent data taken at 25 and 40 °C, respectively. The light scattering measurements were made on dilute samples with $C \sim 10^{-5}$ g/mL. The dashed lines separate regions of sufficient (II) and insufficient (I and III) cross-linking.

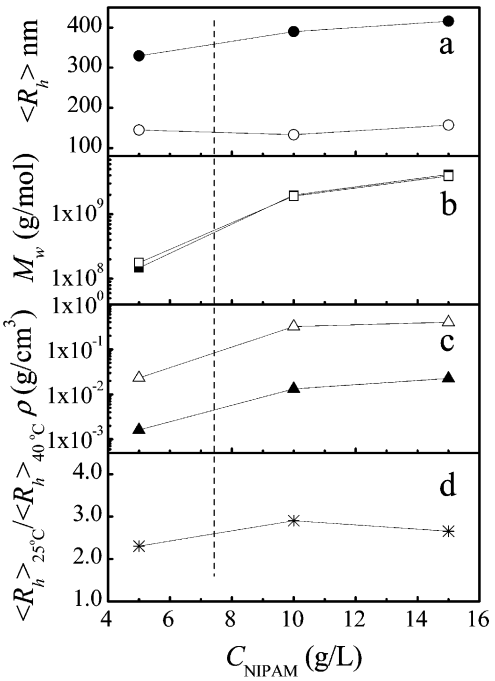

Figure 3. (a) $\langle R_h \rangle$, (b) M_w, (c) ρ, and (d) $\langle R_h \rangle_{25°C}/\langle R_h \rangle_{40°C}$ of particles produced as a function of the initial C_{NIPAM} at a constant initial C_{KPS} of 400 mg/L and a constant T_{syn} of 70 °C. The solid and open symbols represent data taken at 25 and 40 °C, respectively. Light scattering measurements were made on dilute samples with $C \sim 10^{-5}$ g/mL. The dashed line separates regions of sufficient (right side) and insufficient (left side) cross-linking.

Influence of the Reaction Conditions. The formation of self-cross-linked gel nanospheres was investigated systematically as functions of the reaction temperature T_{syn}, initial NIPAM monomer concentration C_{NIPAM}, and initial KPS initiator concentration C_{KPS}.

The production of self-cross-linked microgels was first investigated at different reaction temperatures, while the initial concentrations of NIPAM and KPS were kept at 10 g/L and 400 mg/L, respectively. Different reaction times, as are specified in Table 1, were used to ensure the completion of the monomer conversion. Figure 2 shows how the average hydrodynamic radius $\langle R_h \rangle$, molar mass M_w, solid density ρ, and swelling ratio $\langle R_h \rangle_{25°C}/\langle R_h \rangle_{40°C}$ change with the reaction temperature. The data can be discussed in terms of three temperature regions, as are shown separated by dashed lines in Figure 2: (I) $T_{syn} <$ 52 °C, (II) 52 < T_{syn} < 78 °C, and (III) $T_{syn} >$ 78 °C. Only in region II were the measured values of M_w at 25 and 40 °C consistent. In both of the other regions, the values of M_w measured at 40 °C were higher than those measured at 25 °C. We interpret the observation of higher M_w values at 40 °C than at 25 °C as a sign of insufficient cross-linking; it has been shown[21] that, if cross-linking is insufficient, free chains will pack or adsorb onto existing gel spheres or associate to form aggregates when the temperature is above the LCST but will dissociate below the LCST, leading to a change in the average M_w of the particles.

In region II, where the values of M_w measured below and above the LSCT are consistent and we believe that sufficient cross-linking has occurred, M_w, $\langle R_h \rangle_{25°C}$, and $\langle R_h \rangle_{40°C}$ all decrease with an increasing reaction temperature. The ratio of $\langle R_h \rangle_{25°C}/\langle R_h \rangle_{40°C}$ changes little in this region, falling between 3.0 and 2.8. The high ratio of $\langle R_h \rangle_{25°C}/\langle R_h \rangle_{40°C}$ results in a large difference in the solid density of the gel spheres below and above the LCST. The solid density ρ of the gel spheres measured at 40 °C decreases from 0.48 to 0.32 g/cm^3 as the reaction temperature is increased, whereas that measured at 25 °C decreases from 0.023 to 0.013 g/cm^3. Above 80 °C in region III, these trends continue, except that the molar mass measured at 40 °C is higher than that at 25 °C, indicating that not all of the linear chains have been cross-linked.

At temperatures below about 50 °C, both the polymerization and the cross-linking rates were reduced. Batch 062, synthesized at 39 °C, showed only minimal evidence of monomer conversion into polymers. The value of M_w measured at 25 °C was only 1.4×10^5 g/mol, indicating no gel particle formation. In batch 055, synthesized between 42 and 43 °C, the M_w values were 3.9×10^6 and 6.2×10^7 at 25 and 40 °C, respectively, possibly indicating minimal particle formation, where the different values of M_w measured at the two temperatures again indicates the packing or aggregation of free chains. Only in batch 054, synthesized between 48 and 49 °C, is there clear evidence of stable particle formation by self-cross-linking; here, the values for both M_w and $\langle R_h \rangle$ are high, though the increase in M_w upon heating the solution to 40 °C indicates some packing or aggregation of un-cross-linked polymer chains. This lower limit for stable particle formation is slightly lower than that reported by other authors.[22]

The influence of the monomer concentration C_{NIPAM} on self-cross-linking is shown in Figure 3 where $\langle R_h \rangle$, M_w, ρ, and the ratio $\langle R_h \rangle_{25°C}/\langle R_h \rangle_{40°C}$ are plotted as functions of C_{NIPAM} for polymerization at the standard reaction temperature of 70 °C and constant a C_{KPS} of 400 mg/L. As

(21) Chan, K.; Pelton, R.; Zhang, J. *Langmuir* **1999**, *15*, 4018.

(22) Tam, K. C.; Wu, X. Y.; Pelton, R. H. *J. Polym. Sci., Part A: Polym. Chem.* **1993**, *31*, 963.

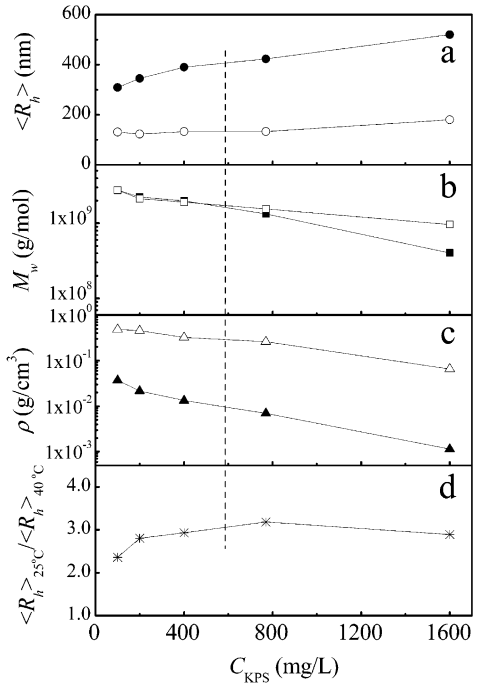

Figure 4. (a) $\langle R_h \rangle$, (b) M_w, (c) ρ, and (d) $\langle R_h \rangle_{25°C}/\langle R_h \rangle_{40°C}$ of particles produced as a function of the initial C_{KPS} at a constant initial C_{NIPAM} of 10 g/L and a constant T_{syn} of 70 °C. The solid and open symbols represent data taken at 25 and 40 °C, respectively. Light scattering measurements were made on dilute samples with $C \sim 10^{-5}$ g/mL. The dashed line separates regions of sufficient (left side) and insufficient (right side) cross-linking.

C_{NIPAM} increases from 5 to 15 g/L, $\langle R_h \rangle_{25°C}$, M_w, and ρ all increase. The data for the molar mass for batch 039 made with a C_{NIPAM} of 5 g/L show insufficient self-cross-linking; the dashed line on Figure 3 indicates that the threshold for sufficient self-cross-linking lies between 5 and 10 g/L, and we have not determined its precise location. At an even lower C_{NIPAM} of 1 g/L, no particles were observed.

The influence of the initiator concentration C_{KPS} on self-cross-linking was studied at a constant initial C_{NIPAM} of 10 g/L and a constant reaction temperature T_{syn} of 70 °C. As is shown in Figure 4, $\langle R_h \rangle_{25°C}$ increases while M_w and ρ both decrease with C_{KPS} for the range of C_{KPS} values studied. At the lowest C_{KPS} value used (50 mg/L in batch 058), a density of 0.042 g/cm^3 was measured at 25 °C, the highest value obtained for self-cross-linked swollen particles in this work; this value is higher than that observed in BIS cross-linked gels.[18] To the right of the dashed line in Figure 4, a region of high C_{KPS} is observed, where M_w at 40 °C is higher than that at 25 °C, indicating that insufficient self-cross-linking has occurred.

The trends observed in the data shown in Figures 2−4 can be discussed in terms of the ratio of free radicals to monomers. In Figure 2, this ratio increases with the temperature; while the total concentration of KPS is constant, the number of free radicals available increases with the temperature. In Figure 3, the ratio decreases as C_{NIPAM} is increased. The trends in these two figures are then the same; $\langle R_h \rangle_{25°C}$, M_w, and ρ all decrease as the ratio of free radicals to monomers increases. The exception to this behavior is shown in Figure 4, where the ratio increases as C_{KPS} increases; while both M_w and ρ decrease, an *increase* in $\langle R_h \rangle_{25°C}$ is observed. This ratio also appears to be important in defining the regions where sufficient self-cross-linking occurs. The threshold for sufficient cross-linking, as is indicated by a dashed line in both Figures 3 and 4, corresponds to a ratio of C_{KPS} to C_{NIPAM} of approximately 0.06.

An explanation of these trends can be found in the principles of surfactant-free emulsion polymerization and colloidal stability.[23] In surfactant-free conditions, an ionic initiator such as KPS not only initiates polymerization but also acts as the source of charge required to stabilize the aggregate particles and a source of ionic strength. When the KPS is added to the reaction mixture, it dissociates into its ionic constituents, some of which decompose into ionic free radicals $SO_4^{\cdot -}$. The sulfate groups are incorporated into the polymer chains, providing the surface charge required to stabilize the particles. The particles grow by association of PNIPAM chains until they reach a surface potential ψ high enough to prevent further association of the chains and coagulation between the particles.

A few simple relations can be used to discuss the trends observed in Figures 2−4 in the regions where effective self-cross-linking occurs. An aggregate sphere of radius R made up of N_c precursor chains, each having average molar mass M_c and carrying some average number of charged groups, will have a surface charge density per particle σ given by

$$\sigma \propto N_c/R^2 \tag{3}$$

This relationship can be written in terms of N_c, M_c, and the solid density of the aggregate ρ_a

$$\sigma \propto N_c^{1/3}(\rho_a/M_c)^{2/3} \tag{4}$$

because $M_w = N_c M_c = {}^4/_3\pi\rho_a R^3 N_A$. The surface potential ψ depends on the surface charge density σ and the Debye screening length κ^{-1} and is given, approximately, by[24]

$$\psi \propto \sigma/\kappa \tag{5}$$

Because the Debye screening length is inversely proportional to the square root of the concentration of the screening ions [I], this equation can be rewritten as

$$\psi \propto \sigma/[I]^{1/2} \tag{6}$$

The chains will aggregate until ψ is large enough to prevent further association. For cases where [I] is constant, the surface charge density σ alone, as is given by eq 4, is sufficient to determine when the particles reach their stable sizes.

For the reaction batches shown in Figures 2 and 3, an increase in the molar ratio of free radicals to monomers leads to a decrease in M_c and an increase in the total number of chains. From eq 4, a constant σ for smaller M_c values also means that N_c, the average number of associated chains inside each sphere, will be smaller. Here, we have neglected changes in the aggregate density because the association of the chains occurs at temperatures well above the LCST, where the aggregates exist in a highly collapsed state. As a result of smaller M_c and N_c values, the molar mass M_w should decrease significantly as the ratio of free radicals to monomers is increased, as is observed in the trends shown in Figures 2 and 3. A careful examination of the density data shown in Figures 2 and 3 does reveal small decreases in the solid density as the ratio of free radicals to monomers increases. An important aspect of the particle formation is the incor-

(23) Gilbert, R. G. *Emulsion Polymerization, a Mechanistic Approach*; Academic Press: London, 1995.
(24) Peach, S. *Macromolecules* **1998**, *31*, 3372.

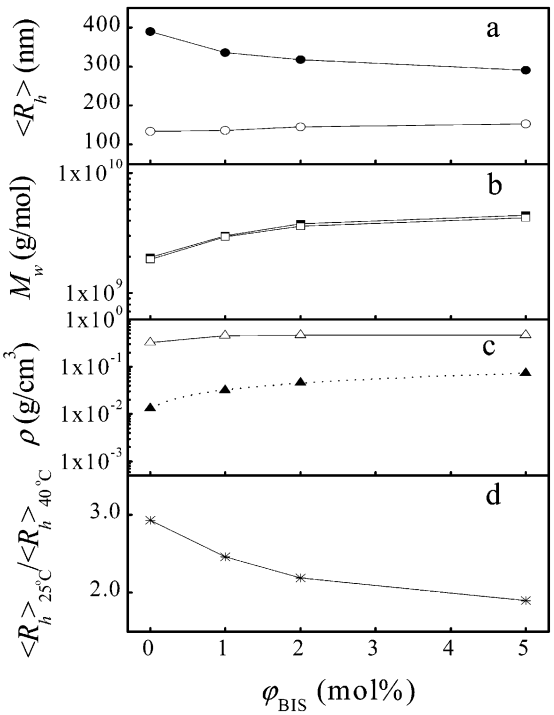

Figure 5. (a) $\langle R_h \rangle$, (b) M_w, (c) ρ, and (d) $\langle R_h \rangle_{25°C}/\langle R_h \rangle_{40°C}$ of particles produced as a function of the initial molar ratio of BIS to NIPAM (φ_{BIS}) at a constant initial C_{NIPAM} of 10 g/L, constant initial C_{KPS} of 400 mg/L, and constant T_{syn} of 70 °C. The solid and open symbols represent data taken at 25 and 40 °C, respectively. Light scattering measurements were made on samples with concentrations $C \sim 10^{-5}$ g/mL. The dashed line is a fit of eq 7 to the data.

poration of the ionic groups SO_4^- into the polymer chains and polymer chain networks. As the ratio of free radicals to monomers increases, the concentration of the covalently bound ionic groups increases, leading to an increase in the hydrophilicity of the particles. This results in a decrease of the solid density ρ of the gel particles when they are diluted, especially at temperatures below the LCST. Both Figures 2 and 3 clearly show this trend. An extreme case was seen in batch 034 where no particles were observed; we believe that the weight ratio of KPS to NIPAM was so high that the polymer chains were simply too hydrophilic to associate in water even at 70 °C. As is seen in both Figures 2 and 3, the particle size $\langle R_h \rangle$ tends to decrease as the ratio of free radicals to monomers increases, confirming that the change in M_w, rather than the change in ρ, dominates the change in $\langle R_h \rangle$.

For the data shown in Figure 4, both the ratio of decomposed KPS to NIPAM and the ionic strength increase as C_{KPS} is increased. Again, we expect that an increase in the molar ratio of free radicals to monomers should lead to a decrease in M_c; however, the increasing ionic strength will mean that a higher N_c, and hence M_w, is expected to satisfy eq 6. Although in Figure 4 the trend of M_w is still the same as that seen in Figures 2 and 3, the change of M_w with C_{KPS} is not as large as it would be if there were no screening effect. This can be seen by comparing the molar masses of the particles made with 15 g/L NIPAM and 400 mg/L KPS (batch 050), as is shown in Figure 3, to the trends of those at lower C_{KPS} (batches 046 and 047), as shown in Figure 4. The M_w values in Figure 4 for concentrations below 400 mg/L KPS, corresponding to a lower ionic strength, are lower. A decrease in $\langle R_h \rangle$ might be expected to accompany this decrease in M_w, which is not observed in Figure 4. However, the radius is measured at a low concentration, where the surface charge is no longer screened and a further swelling of the particles is expected. The trends of an increasing radius and a decreasing density with a higher C_{KPS} are a consequence of the incorporation of more charge into the particles.

These results can be compared to studies of the synthesis of surfactant-free polystyrene nanospheres[25] and PNIPAM chain aggregates.[21] In these studies, the volume of the particles was observed to increase linearly with the initial monomer concentration and polymer chain concentration, respectively. The radii of the polystyrene nanospheres were also observed to increase as the initiator (KPS) concentration increased, but the change of M_w was not recorded.

Cross-Linking Characterization. We investigated the extent of self-cross-linking by using a standard synthesis of PNIPAM gel spheres that includes the addition of a standard cross-linker, BIS. In Figure 5, $\langle R_h \rangle$, M_w, ρ, and $\langle R_h \rangle_{25°C}/\langle R_h \rangle_{40°C}$ are plotted for samples made of 0, 1, 2, and 5 mol % BIS to NIPAM φ_{BIS}. As φ_{BIS} increases, M_w and ρ increase, and the gel spheres become less swollen at 25 °C. This is consistent with other work on PNIPAM microgels and the idea that increased BIS cross-linking leads to a higher gel density.[9]

Theoretically, it is possible to calculate the cross-linking density in terms of the number of repeat units between the neighboring cross-linking points, using the Huggins parameter[10,26] or other treatments.[12] Here, we simply use the solid density of the gel spheres at 25 °C as an indication of the amount of cross-linking to estimate the extent of self-cross-linking. We fit a function of the form

$$\rho = A(\varphi_{BIS} + \varphi_o)^n \qquad (7)$$

to the data points of Figure 5 for the solid density at 25 °C, where φ_o is the self-cross-linking contribution. We obtained values of $\varphi_o = 0.25 \pm 0.08$, A (wt %) $= 2.9 \pm 0.2$, and $n = 0.56 \pm 0.04$. This implies that, under standard reaction conditions, self-cross-linking occurs at a rate corresponding to $\varphi_{BIS} = 0.25$ mol %.

Conclusions

Results of the systematic synthesis and light scattering characterization of self-cross-linked PNIPAM microgels have been presented. The particle size $\langle R_h \rangle$, molar mass M_w, and solid density ρ of the gel spheres have been investigated at 25 and 40 °C, below and above the LCST of PNIPAM, respectively, as functions of the reaction temperature T_{syn}, initial monomer concentration C_{NIPAM}, and initial initiator concentration C_{KPS}. We found suitable ranges of T_{syn}, C_{NIPAM}, and C_{KPS} in which effective self-cross-linking can occur. In general, sufficient cross-linking was observed in samples where the solid content was greater than 30 wt % at 40 °C or 1.3 wt % at 25 °C. The formation of self-cross-linked chain networks requires that the local polymer chain concentration be high enough or, equivalently, the distance between the neighboring chains or chain segments be short enough so that there is a finite probability of *tert*-C free-radical propagation or termination occurring. We observe that regions of insufficient cross-linking correspond to regions where the molar ratio of KPS to NIPAM is high so that the polymer chains are highly charged and very hydrophilic; the exceptions are the cases of low-temperature synthesis where very little decomposed KPS is available for polymerization, let alone cross-linking. For samples made under standard reaction

(25) Zhang, W. M.; Gao, J.; Wu, C. *Macromolecules* **1997**, *30*, 6388.
(26) Flory, P. J. *Principles of Polymer Chemistry*; Cornell University Press: New York, 1953.

conditions, ratios of C_{KPS} to C_{NIPAM} less than ~0.06 are required for the formation of self-cross-linked particles. Comparison of data for self-cross-linked and BIS-cross-linked gel spheres indicates that self-cross-linking under standard reaction conditions occurs at a rate equivalent to the addition of 0.25 mol % BIS. It is important to note that the presence of intrinsic self-cross-linking under standard reaction conditions means that the actual degree of cross-linking that occurs in BIS-cross-linked particles is systematically higher than previously thought. Consistent with lower cross-linking, the swelling ratio for self-cross-linked spheres is generally higher than that for BIS-cross-linked spheres. The ratio of the radii $\langle R_h \rangle_{25°C}/\langle R_h \rangle_{40°C}$ lies in a range between 2.8 and 3.0 and is generally highest in regions where the solid content is the lowest.

In this work, neither surfactant nor cross-linker is introduced. Only interchain self-cross-linking is involved in the formation of polymer chain networks. As cross-linker-free and surfactant-free particles, these slightly cross-linked soft PNIPAM microgels are more closely related to PNIPAM and may be used as standard particles to study the PNIPAM chain and PNIPAM gel phase transitions and the interactions between PNIPAM and many other materials such as surfactants,[27] salts,[28] and solvents.[29] The particle size lies in a convenient and tunable submicron size range, which is ideal for studying the angular dependence of the scattered light, internal motion,[30] and other optical phenomena.

Acknowledgment. This work was supported by the Natural Science and Engineering Research Council of Canada.

LA034207S

(27) Wu, C.; Zhou, S. *J. Polym. Sci., Part B: Polym. Phys.* **1996**, *34*, 1597.
(28) Routh, A. F.; Vincent, B. *Langmuir* **2002**, *18*, 5366.
(29) Costa, R. O. R.; Freitas, R. F. S. *Polymer* **2002**, *43*, 5879.
(30) Wu, C.; Zhou, S. *Macromolecules* **1996**, *29*, 1574.